various tissues from 10 min to 72 h after nasal administration of [^{111}In]-BoHc/A. The [^{111}In]-BoHc/A was detected in the nasal cavity as early as 10 min and remained for at least 24 h after administration. The highest level of radioactivity was found in feces sampled 6 h after nasal administration (Fig. 2*D*). No evidence for the deposition of [^{111}In]-BoHc/A in the CNS was found. The accumulated BoHc/A in the cerebrum and OB were <0.01 and <0.1 SUV for the entire examination period from 10 min to 48 h after nasal administration of 1×10^6 cpm per 18 μl (9 μl, each nostril) [^{111}In]-BoHc/A per mouse, respectively (Fig. 2*E*). On the contrary, [^{111}In]-cholera toxin was detected in the OB from 6 h after nasal administration of 1×10^6 cpm per 20 μl (10 μl, each nostril) [^{111}In]-cholera toxin per mouse (Fig. 2*F*). This finding is in complete agreement with the data obtained with [^{18}F]-BoHc/A (Fig. 2*B*). Radioactive material in samples extracted from the nasal mucosa 10 min to 24 h after administration and subjected to size-exclusion chromatography analysis by using PD-10 columns was found mostly in the high m.w. fractions at 6 h and then gradually appeared in the low m.w. fractions (Fig. 3*B*). This finding suggests that intact BoHc/A molecules were attached to the nasal mucosa for at least the first 6 h after administration. Radioactivity was found in the low m.w. fractions of urine and feces samples at 6 h after nasal administration, suggesting that the vaccine Ags were degraded.

Nasal immunization with BoHc/A induces protective immunity against BoNT/A in nonhuman primates

Nasal immunization of mice, but not macaques, with BoHc/A can induce protective immunity against BoNT/A (12). To investigate whether the recombinant BoHc/A nasal vaccine induces protective immunity, we nasally immunized three cynomolgus macaques with 500 μg BoHc/A, and we administered to one cynomolgus macaque PBS as a control (Fig. 4*A*). Ag-specific Ab responses were assessed by using BoNT/A as a coating Ag for ELISAs. After nasal immunization, the BoNT/A-specific serum IgG Ab titers increased in all BoHc/A-vaccinated macaques, but not in the

A

Monkey (age, sex)	Nasal immunization
#001 (5 years, female)	BoHc/A (500 μg)
#002 (5 years, female)	BoHc/A (500 μg)
#003 (5 years, female)	BoHc/A (500 μg)
#004 (5 years, female)	PBS

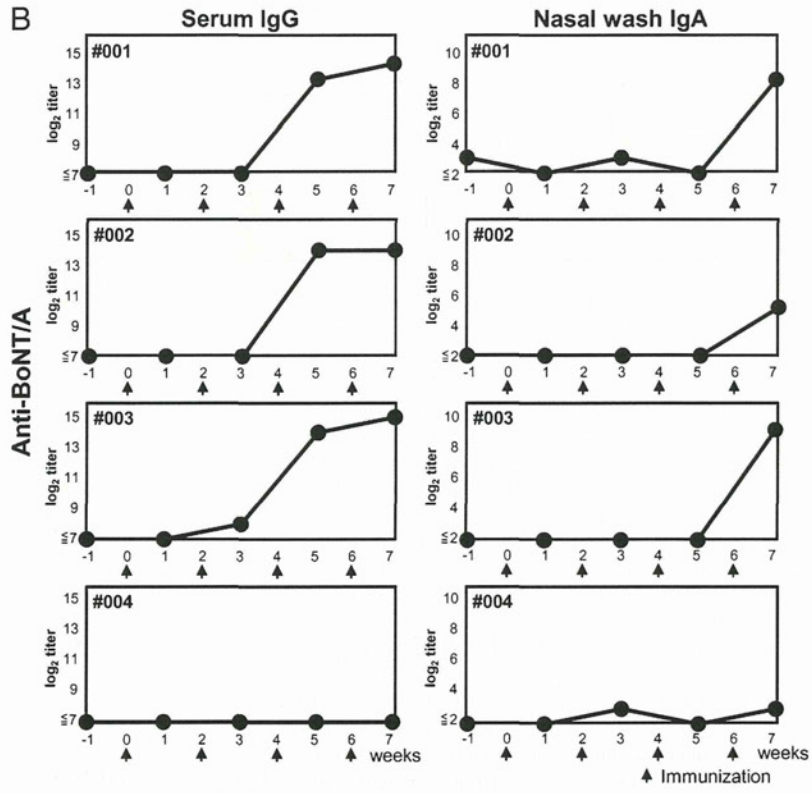

FIGURE 4. Nasal immunization with BoHc/A induces protective immunity in nonhuman primates. *A*, Details for cynomolgus macaques used in the experiment and the dose of BoHc/A used for immunization are shown in this table. *B*, Each cynomolgus macaque was nasally immunized with 500 μg BoHc/A at the times indicated with arrows, serum and nasal wash were collected (indicated by circles), and then Ag-specific IgG Ab in serum (*left*) and IgA Ab in nasal wash (*right*) were measured by the toxin-specific ELISA. *x*-axis indicates time (week) before and after immunization of BoHc/A. *C*, Nasally immunized cynomolgus macaques and one control were challenged systemically with 25 μg (2.7×10^6 LD_{50}) BoNT/A/kg body weight and routinely monitored for 30 d after challenging. All cynomolgus macaques, except the control, were completely protected against the lethal toxin challenge without any clinical signs of disease for 30 d. One control macaque showed onset of the disease as early as 4 h after the challenge and was humanely euthanized.

control macaque administered PBS. In addition, the toxin-specific secretory IgA Ab titers in nasal washes increased in all the nasally immunized macaques, but not in the control macaque (Fig. 4*B*). These results indicated that BoHc/A is a highly immunogenic nasal vaccine capable of inducing toxin-specific Abs not only in systemic compartments but in mucosal compartments in cynomolgus macaques.

Next, a challenge test with 25 μg (2.7×10^6 LD_{50}) BoNT/A per kilogram body weight was performed on all three BoHc/A-vaccinated macaques and on the one control macaque; the dosage required was estimated from the neutralizing activity in serum from the immunized macaques (Supplemental Fig. 4). The BoHc/A-vaccinated macaques, but not the control, were completely protected against the high lethal dose of i.p. injected BoNT/A (Fig. 4*C*). There were no clinical signs of toxin-associated disease over the 30-d observation period after the BoNT/A challenge test. The control macaque was euthanized 4 h after the challenge because of the development of several clinical signs of botulism. After 30 d, all BoHc/A-vaccinated macaques that had undergone the challenge test were sacrificed. Detailed examinations revealed the absence of any clinical signs of organ abnormality or botulism. Taken together, these results demonstrate that the nasal BoHc/A vaccine is a safe and effective mucosal vaccine against *C. botulinum* neurotoxin.

Adaptation of PET/MRI in vivo molecular imaging for tissue distribution analysis of nasally administered [^{18}F]-BoHc/A in nonhuman primates

Because we confirmed that the nasal immunization of macaques with BoHc/A induced protective immunity, we then investigated whether the nasal BoHc/A vaccine is transported to the CNS via the OB in nonhuman primates using two naive rhesus macaques on the different experiment. To ensure that the [^{18}F]-BoHc/A completely penetrated the nasal cavity and the olfactory epithelium, we laid two macaques (No. 5 and 6) on their backs for 10 min after the nasal administration of 34.5 and 54.7 MBq [^{18}F]-BoHc/A in 315 and 500 μl PBS, respectively. After anesthesia, the macaque's head was placed into the PET scanner system and real-time imaging was performed for 6 h. To confirm the exact position of the cerebrum, we performed an MRI scan and then superimposed the PET images onto the MRI images. Real-time PET images of macaque No. 6, from 15 min to 6 h after nasal administration, are shown in Fig. 5*A*. No CNS deposition of vaccine Ags in cerebrum was detected within 6 h after nasal administration of [^{18}F]-BoHc/A in either macaque. To confirm the absence of [^{18}F]-BoHc/A in the cerebrum of the two macaques, we directly counted radioactivity in each tissue, including cerebrum and OB, at 6 h after immunization (Fig. 5*B*, 5*C*). We found that the accumulated [^{18}F]-BoHc/A in the cerebrum and OB were <0.01 and <0.04 SUV, respectively. Taken together, these results demonstrated that there was no CNS deposition of nasally administered BoHc/A vaccine in the rhesus macaques. Six hours after nasal administration of [^{18}F]-BoHc/A, radioactivity was detected in the urine, stomach, kidney, small intestine, and nasal mucosa (Fig. 5*B*). Among these samples, the highest level of radioactivity was found in the urine. The radioactivity in urine was found in the low m.w. fractions after size-exclusion chromatography analysis by using a PD-10 column (Fig. 3*A*), suggesting that degradation of [^{18}F]-BoHc/A had occurred.

Discussion

Radio- or luminescence-labeling techniques have the capacity to track vaccine Ags and adjuvants (3, 23). However, these classical

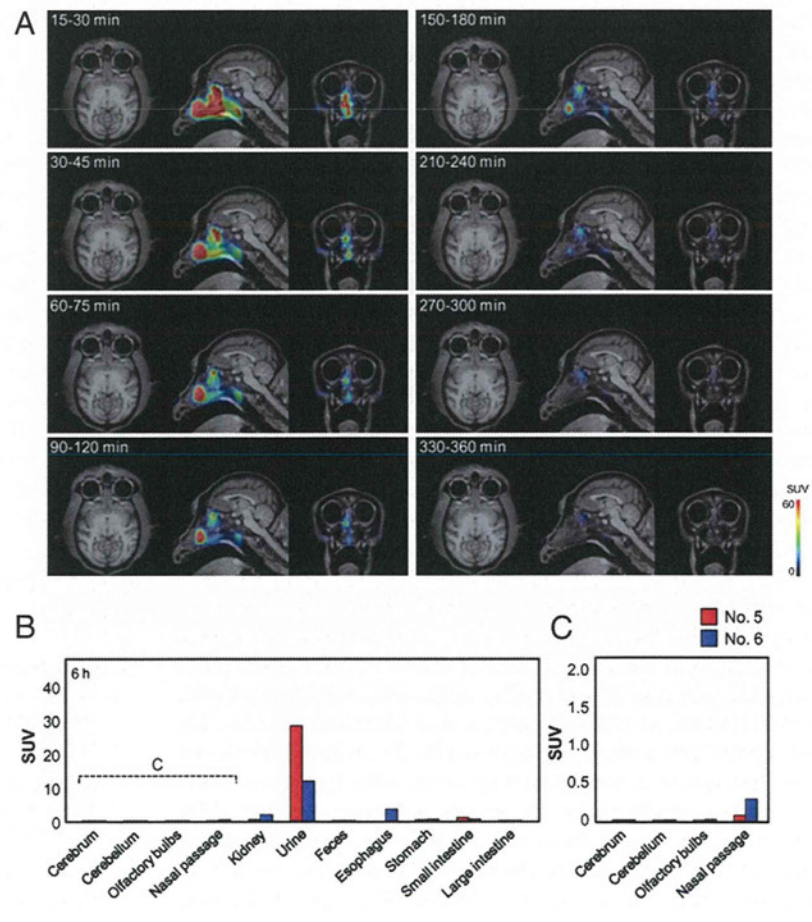

FIGURE 5. PET/MRI (*A*) and SUV (*B*) after nasal administration of [^{18}F]-BoHc/A in nonhuman primates. *A*, After administration of [^{18}F]-BoHc/A into a nostril of naive rhesus macaque No. 6, the macaque's head was scanned for 6 h by using a PET scanner. Real-time PET images overlaid on MRI images are shown for the indicated times postimmunization. Although deposition of [^{18}F]-BoHc/A in nasal cavity was detected within 6 h, no CNS deposition of [^{18}F]-BoHc/A in cerebrum was detected within 6 h after administration of [^{18}F]-BoHc/A. *B*, At the 6-h time point, [^{18}F] radioactivity in each tissue from the two rhesus macaques, No. 5 and 6, was directly counted and expressed as an SUV. *C*, To further check whether there is an accumulation in the CNS, we enlarged the SUV scale for cerebrum, cerebellum, and OBs to focus on levels near the detection limit.

methods are generally end-point approaches because they require the use of multiple animals for diachronic analysis. In this paper, we showed that quantitative real-time analysis of the tissue distribution and degradation of nasal vaccines could be achieved in both rodents and nonhuman primates. To evaluate the safety of the nasal vaccine candidate against *C. botulinum* neurotoxin, BoHc/A, we developed an in vivo molecular imaging system for ADME by using [^{18}F]-BoHc/A and PET together with CT or MRI and the use of PPIS. Our data from in vivo molecular imaging with [^{18}F]-BoHc/A was consistent with the results obtained by classical direct counting to measure the radioactivity in various tissues in mice and nonhuman primates. Thus, our in vivo molecular imaging system is a potentially important strategy for the precise analysis of nasal vaccines and adjuvants for preclinical safety testing in individual animals.

After the nasal administration of [^{18}F]-BoHc/A to mice, a major portion of [^{18}F]-BoHc/A immediately adhered to the nasal mucosa and, simultaneously, some Ag was cleared from the nasal cavity by the mucociliary clearance mechanism (4) and was transported to the throat, esophagus, gastrointestinal tract (including the stomach and intestine), and urinary bladder in order of decreasing abundance (Fig. 1*A*, Supplemental Videos 1 and 2, and Supplemental Fig. 3). We used our PET imaging method to identify the sites of accumulated [^{18}F]-BoHc/A in real time after nasal administration and to quantify the amounts of accumulated [^{18}F]-BoHc/A (Fig. 1*B*). We confirmed the accuracy of this approach by comparing these data with those derived by the classical direct counting assay on various dissected tissues (Fig. 2*A*). Because radioactive material with a low m.w. was found in the stomach and intestine, as well as in the feces, we suggest that the portion of nasal [^{18}F]-BoHc/A or [^{111}In]-BoHc/A vaccine that reached the digestive tract was degraded and then absorbed in the intestines (Fig. 3*A*, 3*B*). Radioactive material with a low m.w. was also found in the urine. Because [^{18}F]-BoHc/A and [^{111}In]-BoHc/A were synthesized by labeling N-terminal and ε–Lys amino groups on BoHc/A, nasally administered [^{18}F]-BoHc/A or [^{111}In]-BoHc/A might be degraded in the gastrointestinal tract and converted to [^{18}F]-ε –Lys or [^{111}In]-ε –Lys, which undergo fast blood clearance via the kidneys. Many [^{111}In]-glycoproteins administered to rodents are degraded and converted to [^{111}In]-ε –Lys, which is then recovered in urine and feces (24). Most of the low m.w. compounds labeled with [^{111}In] were detected in feces at 6 h after nasal administration (Fig. 2*D*), whereas most of the low m.w. compounds labeled with [^{18}F] were present in urine (Fig. 2*A*). This finding suggests that the [^{18}F]-compounds are absorbed from the gastrointestinal tract and cleared by the kidneys into the urine at a faster rate than is the case for the [^{111}In] compounds. In addition, we found no indication of accumulated radioactivity in bones in mice nasally administered [^{18}F]-BoHc/A (Fig. 2*A*). Because [^{18}F] fluoride accumulates in bone (25), our observation suggests that degradation of [^{18}F]-BoHc/A to [^{18}F] fluoride did not occur.

The radioactive material detected in the nasal mucosa that was derived from [^{18}F]-BoHc/A or [^{111}In]-BoHc/A was high m.w., suggesting the maintenance of the intact nasal vaccine for as long as 6 h after nasal administration (Fig. 3*A*, 3*B*). Although BoHc/A degraded gradually on the surface of the nasal epithelium and/or within the nasal cavity beginning 6 h after administration (Fig. 3*B*) by contact with proteolytic enzymes (26, 27), intact BoHc/A can bind and penetrate the mucosal epithelial cells by a transcytosis mechanism mediated by an as yet unknown receptor (28). Therefore, we propose that some of the BoHc/A taken up by and released from the nasal epithelium might stimulate the airway immune system and lead to the induction of Ag-specific immune responses. In fact, we demonstrated the induction of toxin-specific systemic IgG and mucosal IgA Ab responses with strong Ag neutralizing activity when macaques were nasally immunized with 500 μg BoHc/A (Fig. 4*B*). In addition, we performed a toxin challenge test to provide proof of efficacy of the nasal BoHc/A vaccine in nonhuman primates (Fig. 4*C*). All the macaques that received the nasal BoHc/A vaccine were protected from an i.p. challenge with a dose of BoNT/A (25 μg [2.7×10^6 LD_{50}]/kg), which is ~35,000 times the lethal dose of ~0.7 ng/kg (29).

Recent nasal vaccine studies have raised concerns about the deposition and accumulation of candidate vaccine Ags in the CNS through direct transport from nasal mucosa to the cerebrum via the OB (1, 3). For this reason, we investigated the deposition and accumulation of the nasal BoHc/A vaccine by direct tissue counting analyses of [^{18}F]-BoHc/A or [^{111}In]-BoHc/A in mice. We showed that there was no OB deposition or accumulation of BoHc/A in the CNS within 6 h (≤0.04 SUV by [^{18}F] counts) or 48 h (≤0.1 SUV by [^{111}In] counts) after nasal administration (Fig. 2*B*, 2*D*). These results demonstrate that the nasal BoHc/A vaccine did not reach the mouse CNS, despite the large surface area of the nasal cavity containing olfactory epithelium that is connected to the CNS (4), and thereby confirm the safety of the vaccine. On the basis of these promising findings for the efficacy of the nasal BoHc/A vaccine in mice, we used rhesus macaques as a nonhuman primate model to perform the preliminary experiments necessary to validate the approach for future human trials. Using the [^{18}F]-BoHc/A–PET in vivo molecular imaging method, we showed that there was no [^{18}F]-BoHc/A deposited in the cerebrum of rhesus macaques 6 h after nasal administration of 57.4 MBq [^{18}F]-BoHc/A (Fig. 5*A*). Furthermore, 6 h after nasal administration of [^{18}F]-BoHc/A, no [^{18}F] radioactivity was detected in the cerebrum or OB of the macaque by direct tissue counting (Fig. 5*C*). Thus, we showed that there is no deposition of the Ag in the CNS in nonhuman primates. This result confirms our results in mice and shows that nasal delivery of BoHc/A is safe with respect to its ADME profile. In addition, the radioactivity in various tissues of the macaques after nasal administration of [^{18}F]-BoHc/A were in complete agreement with the data obtained in mice (Figs. 2*A*, 5*B*). Degraded radioactive material with a low m.w. was also found in the urine of macaques (Fig. 3*A*). Taken together, our findings suggest that after nasal administration of [^{18}F]-BoHc/A to macaques, the [^{18}F]-compound is absorbed from the gastrointestinal tract and cleared by the kidneys into the urine.

In summary, we developed an in vivo molecular imaging system that combines PET with CT or MRI and is suitable as an ADME profiling system for biotechnology-derived pharmaceuticals, including nasal vaccines. Using this system, we demonstrated the safety and efficiency of a nasal vaccine candidate against botulism in mice and nonhuman primates. Our in vivo molecular imaging system can be used to replace the current whole-body autoradiography method for the preclinical ADME evaluation and may be suitable for use in human clinical studies.

Disclosures

The authors have no financial conflicts of interest.

References

1. Yuki, Y., and H. Kiyono. 2009. Mucosal vaccines: novel advances in technology and delivery. *Expert Rev. Vaccines* 8: 1083–1097.
2. Mutsch, M., W. Zhou, P. Rhodes, M. Bopp, R. T. Chen, T. Linder, C. Spyr, and R. Steffen. 2004. Use of the inactivated intranasal influenza vaccine and the risk of Bell's palsy in Switzerland. *N. Engl. J. Med.* 350: 896–903.
3. van Ginkel, F. W., R. J. Jackson, Y. Yuki, and J. R. McGhee. 2000. Cutting edge: the mucosal adjuvant cholera toxin redirects vaccine proteins into olfactory tissues. *J. Immunol.* 165: 4778–4782.
4. Illum, L. 2003. Nasal drug delivery—possibilities, problems and solutions. *J. Control. Release* 87: 187–198.

5. Staud, F., M. Nishikawa, K. Morimoto, Y. Takakura, and M. Hashida. 1999. Disposition of radioactivity after injection of liver-targeted proteins labeled with 111In or 125I. Effect of labeling on distribution and excretion of radioactivity in rats. *J. Pharm. Sci.* 88: 577–585.
6. Gross, S., S. T. Gammon, B. L. Moss, D. Rauch, J. Harding, J. W. Heinecke, L. Ratner, and D. Piwnica-Worms. 2009. Bioluminescence imaging of myeloperoxidase activity in vivo. *Nat. Med.* 15: 455–461.
7. Muramatsu, S., T. Okuno, Y. Suzuki, T. Nakayama, T. Kakiuchi, N. Takino, A. Iida, F. Ono, K. Terao, N. Inoue, et al. 2009. Multitracer assessment of dopamine function after transplantation of embryonic stem cell-derived neural stem cells in a primate model of Parkinson's disease. *Synapse* 63: 541–548.
8. Brooks, D. J. 2008. The role of structural and functional imaging in parkinsonian states with a description of PET technology. *Semin. Neurol.* 28: 435–445.
9. Vallabhajosula, S. 2007. (18)F-labeled positron emission tomographic radiopharmaceuticals in oncology: an overview of radiochemistry and mechanisms of tumor localization. *Semin. Nucl. Med.* 37: 400–419.
10. May, A. 2009. New insights into headache: an update on functional and structural imaging findings. *Nat. Rev. Neurol.* 5: 199–209.
11. Yagle, K. J., J. F. Eary, J. F. Tait, J. R. Grierson, J. M. Link, B. Lewellen, D. F. Gibson, and K. A. Krohn. 2005. Evaluation of 18F-annexin V as a PET imaging agent in an animal model of apoptosis. *J. Nucl. Med.* 46: 658–666.
12. Park, J. B., and L. L. Simpson. 2003. Inhalational poisoning by botulinum toxin and inhalation vaccination with its heavy-chain component. *Infect. Immun.* 71: 1147–1154.
13. Boles, J., M. West, V. Montgomery, R. Tammariello, M. L. Pitt, P. Gibbs, L. Smith, and R. D. LeClaire. 2006. Recombinant C fragment of botulinum neurotoxin B serotype (rBoNTB (HC)) immune response and protection in the rhesus monkey. *Toxicon* 47: 877–884.
14. Fujihashi, K., H. F. Staats, S. Kozaki, and D. W. Pascual. 2007. Mucosal vaccine development for botulinum intoxication. *Expert Rev. Vaccines* 6: 35–45.
15. Sakaguchi, G. 1982. *Clostridium botulinum* toxins. *Pharmacol. Ther.* 19: 165–194.
16. Kondo, H., T. Shimizu, M. Kubonoya, N. Izumi, M. Takahashi, and G. Sakaguchi. 1984. Titration of botulinum toxins for lethal toxicity by intravenous injection into mice. *Jpn. J. Med. Sci. Biol.* 37: 131–135.
17. Haka, M. S., and M. R. Kilbourn. 1989. Synthesis and regional mouse brain distribution of [11C]nisoxetine, a norepinephrine uptake inhibitor. *Int. J. Rad. Appl. Instrum. B* 16: 771–774.
18. Tang, G., W. Zeng, Y. Meixiang, and G. Kabalka. 2008. Facile synthesis of N-succnimidyl-4-[^{18}F]fluorobenzoate ([^{18}F]SFB) for protein labeling. *J. Labelled Comp. Radiopharm.* 51: 68–71.
19. Michel, R. B., P. M. Andrews, M. E. Castillo, and M. J. Mattes. 2005. In vitro cytotoxicity of carcinoma cells with 111In-labeled antibodies to HER-2. *Mol. Cancer Ther.* 4: 927–937.
20. Mizuta, T., K. Kitamura, H. Iwata, Y. Yamagishi, A. Ohtani, K. Tanaka, and Y. Inoue. 2008. Performance evaluation of a high-sensitivity large-aperture small-animal PET scanner: ClairvivoPET. *Ann. Nucl. Med.* 22: 447–455.
21. Uchida, H., T. Okamoto, T. Ohmura, N. Shimizu, N. Satoh, T. Koike, and T. Yamashita. 2004. A compact planar poitron imaging system. *Nucl. Instrum. Methods Phys. Res. A* 516: 564–574.
22. Watanabe, M., H. Okada, K. Shumizu, T. Omura, E. Yoshikawa, T. Kosugi, S. Mori, and T. Yamashita. 1997. A high resolution animal PET scanner using compact PS-PMT detectors. *IEEE Trans. Nucl. Sci.* 44: 1277–1282.
23. Hagiwara, Y., Y. I. Kawamura, K. Kataoka, B. Rahima, R. J. Jackson, K. Komase, T. Dohi, P. N. Boyaka, Y. Takeda, H. Kiyono, et al. 2006. A second generation of double mutant cholera toxin adjuvants: enhanced immunity without intracellular trafficking. *J. Immunol.* 177: 3045–3054.
24. Franano, F. N., W. B. Edwards, M. J. Welch, and J. R. Duncan. 1994. Metabolism of receptor targeted 111In-DTPA-glycoproteins: identification of 111In-DTPA-epsilon-lysine as the primary metabolic and excretory product. *Nucl. Med. Biol.* 21: 1023–1034.
25. Grant, F. D., F. H. Fahey, A. B. Packard, R. T. Davis, A. Alavi, and S. T. Treves. 2008. Skeletal PET with 18F-fluoride: applying new technology to an old tracer. *J. Nucl. Med.* 49: 68–78.
26. Hussain, A., J. Faraj, Y. Aramaki, and J. E. Truelove. 1985. Hydrolysis of leucine enkephalin in the nasal cavity of the rat—a possible factor in the low bioavailability of nasally administered peptides. *Biochem. Biophys. Res. Commun.* 133: 923–928.
27. Jørgensen, L., and E. Bechgaard. 1994. Intranasal permeation of thyrotropin-releasing hormone: in vitro study of permeation and enzymatic degradation. *Int. J. Pharm.* 107: 231–237.
28. Ravichandran, E., F. H. Al-Saleem, D. M. Ancharski, M. D. Elias, A. K. Singh, M. Shamim, Y. Gong, and L. L. Simpson. 2007. Trivalent vaccine against botulinum toxin serotypes A, B, and E that can be administered by the mucosal route. *Infect. Immun.* 75: 3043–3054.
29. Gill, D. M. 1982. Bacterial toxins: a table of lethal amounts. *Microbiol. Rev.* 46: 86–94.

LETTERS
PUBLISHED ONLINE: 20 JUNE 2010 | DOI: 10.1038/NMAT2784
nature materials

Nanogel antigenic protein-delivery system for adjuvant-free intranasal vaccines

Tomonori Nochi[1†‡], Yoshikazu Yuki[1†], Haruko Takahashi[2], Shin-ichi Sawada[2], Mio Mejima[1], Tomoko Kohda[3], Norihiro Harada[4], Il Gyu Kong[1], Ayuko Sato[1], Nobuhiro Kataoka[1], Daisuke Tokuhara[1], Shiho Kurokawa[1], Yuko Takahashi[1], Hideo Tsukada[4], Shunji Kozaki[3], Kazunari Akiyoshi[2] and Hiroshi Kiyono[1*]

Nanotechnology is an innovative method of freely controlling nanometre-sized materials[1]. Recent outbreaks of mucosal infectious diseases have increased the demands for development of mucosal vaccines because they induce both systemic and mucosal antigen-specific immune responses[2]. Here we developed an intranasal vaccine-delivery system with a nanometre-sized hydrogel ('nanogel') consisting of a cationic type of cholesteryl-group-bearing pullulan (cCHP). A non-toxic subunit fragment of *Clostridium botulinum* type-A neurotoxin BoHc/A administered intranasally with cCHP nanogel (cCHP-BoHc/A) continuously adhered to the nasal epithelium and was effectively taken up by mucosal dendritic cells after its release from the cCHP nanogel. Vigorous botulinum-neurotoxin-A-neutralizing serum IgG and secretory IgA antibody responses were induced without co-administration of mucosal adjuvant. Importantly, intranasally administered cCHP-BoHc/A did not accumulate in the olfactory bulbs or brain. Moreover, intranasally immunized tetanus toxoid with cCHP nanogel induced strong tetanus-toxoid-specific systemic and mucosal immune responses. These results indicate that cCHP nanogel can be used as a universal protein-based antigen-delivery vehicle for adjuvant-free intranasal vaccination.

Beginning in 2003, an enormous research initiative—Grand Challenges in Global Health—has been organized worldwide with the support of the Bill and Melinda Gates Foundation and the US National Institutes of Health. Its aim is to overcome the global infectious disease problems affecting human health today[3]. The development of a new-generation needle-free mucosal vaccine has been proposed as one of the initiative's most important goals, because it can elicit antigen-specific systemic humoral and cellular immune responses and simultaneously induce mucosal immunity, especially in the aero-digestive and reproductive tracts[2–4]. FluMist, which is composed of cold-adapted trivalent live influenza viruses, is a well-known example as the first advanced intranasal vaccine to be used in US public health, in 2003 (ref. 5). Since then, tremendous efforts have been made to further develop intranasal vaccine technology. Subunit intranasal vaccination is expected to be the safest strategy, because it should have a low risk of causing unfavourable and undesired biological reactions[6]. However, intranasal administration of a subunit antigen alone is generally insufficient for induction of antigen-specific immune responses. As a result, an adjuvant such as a bacterial toxin generally needs to be added, but these toxins are poorly tolerated by humans[7].

Cholera toxin and heat-labile enterotoxin have been extensively used as potent mucosal adjuvants in experimental animal studies because of their multiple immune-potentiating functions: they activate immunocompetent cells, including dendritic cells and B cells, and thus induce antigen-specific mucosal immunity[7–9]. However, a human clinical trial carried out in Switzerland from 2000 to 2001 to develop an intranasal influenza vaccine with inactivated influenza virus combined with a small amount of heat-labile enterotoxin was withdrawn because the co-administered heat-labile enterotoxin was suspected of causing Bell's palsy, a rare condition, in vaccinated subjects[10]. In addition, a separate study in mice demonstrated that the toxin-based adjuvant migrated into, and accumulated in, the olfactory tissues[11]. As a result of these safety issues, the development of intranasal vaccines employing the co-administration of toxin-based adjuvants has rapidly declined. Further scientific and technological innovations that will help the development of safe but effective adjuvant-free intranasal vaccines are, therefore, of high priority in global health.

Application of biomaterials, such as polymer nanoparticles and liposomes, has a great potential in vaccine development and immunotherapy[12–14]. In particular, nanometre-sized (<100 nm) polymer hydrogels (nanogels) have attracted growing interest as nanocarriers, especially in drug-delivery systems[15,16]. We have developed a new method of creating a series of functional nanogels through self-assembly of associating polymers[17]. One of these polymers, the cholesteryl-group-bearing pullulan (CHP) forms physically crosslinked nanogels by self-assembly in water[18–22] (Fig. 1a and Supplementary Fig. S1). The CHP nanogels trap various proteins by mainly hydrophobic interactions[23] and acquire chaperon-like activity because the proteins are trapped inside a hydrated nanogel polymer network (nanomatrix) without aggregating and are gradually released in the native form[20,24]. These properties make the CHP nanogel a superior nanocarrier for protein delivery, especially in the area of cancer vaccine development[25,26]. In fact, recent successful clinical studies have clearly shown that subcutaneous injection of CHP nanogel carrying the cancer antigen HER2 (CHP–HER2) or NY-ESO-1 (CHP–NY-ESO-1) effectively

[1]Division of Mucosal Immunology, Department of Microbiology and Immunology, The Institute of Medical Science, The University of Tokyo, Tokyo 108-8639, Japan, [2]Department of Organic Materials, Institute of Biomaterials and Bioengineering, Tokyo Medical and Dental University, Tokyo 101-0062, Japan, [3]Laboratory of Veterinary Epidemiology, Department of Veterinary Science, Graduate School of Life and Environmental Sciences, Osaka Prefecture University, Osaka 599-8531, Japan, [4]PET Center, Central Research Laboratory, Hamamatsu Photonics K.K., Shizuoka 434-8601, Japan. †These authors contributed equally to this work. ‡Present address: Division of Infectious Diseases, Center for AIDS Research, University of North Carolina, Chapel Hill, North Carolina 27599, USA. *e-mail: kiyono@ims.u-tokyo.ac.jp.

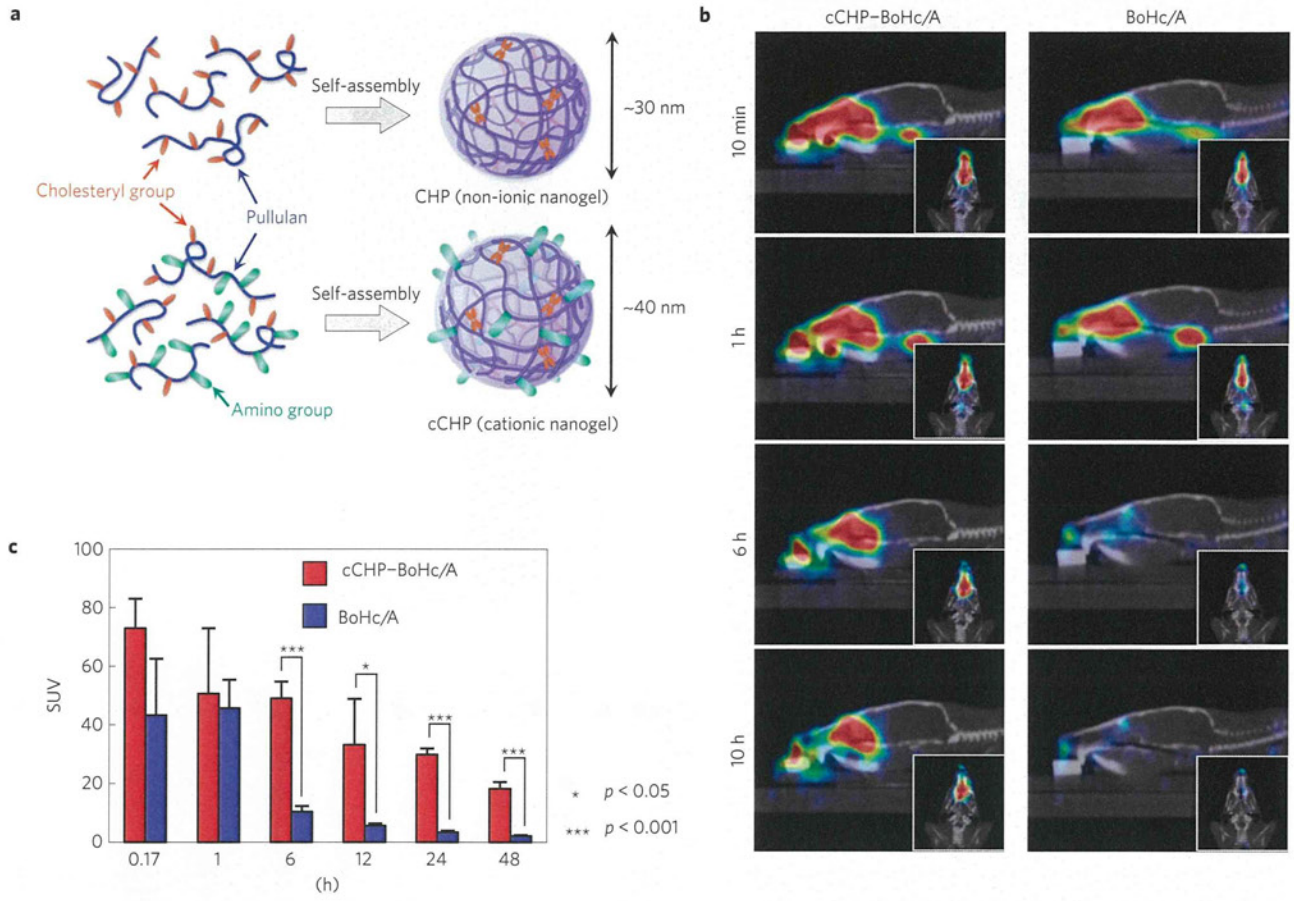

Figure 1 | Use of cCHP nanogel as a new antigen-delivery vehicle for intranasal vaccination. a, cCHP nanogel was generated from a cationic type of cholesteryl-group-bearing pullulan. **b**, Superimposition of sagittal and transverse (photo insets) PET images on the corresponding computed tomography images showed that intranasally administered cCHP nanogels carrying [^{18}F]-labelled BoHc/A were effectively delivered to the nasal mucosa. **c**, Direct quantitative study with [^{111}In]-labelled BoHc/A further demonstrated that BoHc/A was retained in the nasal tissues for more than two days after intranasal immunization with cCHP nanogel. In contrast, most naked BoHc/A disappeared from the nasal cavity within 6 h after administration.

induces antigen-specific CD8$^+$ cytotoxic T lymphocyte responses and antibody production[21,22]. Therefore, the technological successes have been extended to the use of a CHP nanogel strategy to develop adjuvant-free intranasal vaccines that can induce antigen-specific protective immunity against infectious diseases.

To demonstrate the effectiveness of CHP nanogel as a new vehicle for adjuvant-free intranasal vaccines, we prepared and used an *Escherichia-coli*-derived recombinant non-toxic receptor-binding fragment (heavy-chain C terminus) of *C. botulinum* type-A neurotoxin subunit antigen Hc (BoHc/A) as a prototype vaccine antigen because the immunogenicity of BoHc/A has already been demonstrated elsewhere[27,28]. In the initial study for evaluation of BoHc/A quality, because the antigen was highly purified, only a negligible amount of endotoxin with no *in vivo* biological effects on immunocompetent cells was detected (Supplementary Table S1; ref. 29). *C. botulinum* has been defined as a category A bioterrorism agent by the US Centers for Disease Control and Prevention because of the strong neural toxicity of *C. botulinum*-producing neurotoxin (BoNT), which could enable the bacterium to be disseminated as a biological weapon. Thus, the development of an effective vaccine—especially a mucosal vaccine—against BoNT is important for global deterrence of bioterrorism[30].

We intranasally immunized mice with CHP nanogel carrying BoHc/A (CHP–BoHc/A). It should be noted that the levels of endotoxin carried by the CHP nanogel were undetectable (Supplementary Table S1). Subsequent quality analyses of CHP–BoHc/A to confirm the nanometre-scale size uniformity and complex formation by dynamic light scattering (DLS) and fluorescence response energy transfer (FRET) analyses showed that the CHP nanogel continuously formed the nanoparticles after the incorporation of BoHc/A (Supplementary Fig. S2). However, intranasally administered CHP–BoHc/A was no better than naked BoHc/A for inducing BoNT/A-specific antibody responses (Supplementary Fig. S3a,b). These results suggest that CHP–BoHc/A is delivered minimally to the upper respiratory immune system because the mucosal tissues are tightly covered by an epithelial layer. In support of this hypothesis, the use of CHP nanogel did not enhance the BoHc/A uptake by nasal dendritic cells when compared to intranasal administration of naked BoHc/A (Supplementary Fig. S3c). Therefore, we next developed an endotoxin-free cationic type of CHP (cCHP) nanogel containing 15 amino groups per 100 glucose units (Fig. 1a and Supplementary Fig. S1 and Table S1) to improve the antigen-delivery efficacy of CHP nanogel to the anionic epithelial cell layer. DLS and FRET analyses showed that the cCHP nanogel possessed similar structural characteristics to the CHP nanogel because it maintained nanoscale size uniformity even after the incorporation of BoHc/A (Supplementary Fig. S2). In addition, consistent with its positive zeta-potential (Supplementary Table S2), it strongly interacted with the membranes of HeLa cells (Supplementary Fig. S4a) and was subsequently taken up into the cells by endocytosis (Supplementary Fig. S4b). These results are consistent with our previous finding that cCHP nanogel effectively delivered several proteins into cells *in vitro*[31]. Furthermore, an *in vivo*

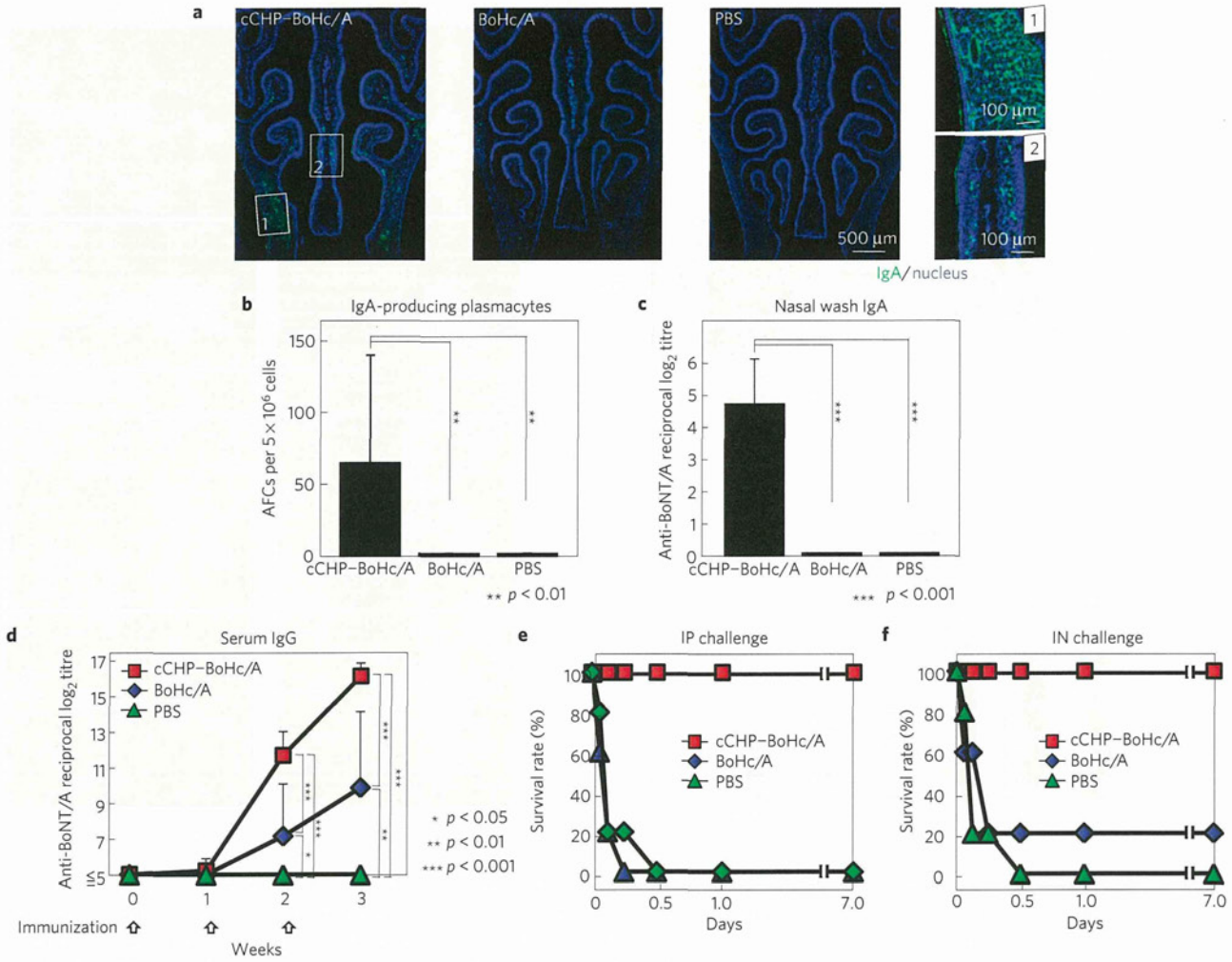

Figure 2 | Efficiency of BoHc/A with cCHP nanogel. a,**b**, BoNT/A-specific IgA-producing cells (or antibody-forming cells: AFCs) were effectively induced and recruited in the lamina propria and paranasal sinuses of the nasal mucosa 1 week after final immunization with cCHP-BoHc/A. **c**, Vigorous BoNT/A-specific IgA antibody responses were observed in nasal washes collected from mice intranasally immunized with cCHP-BoHc/A, but not from those given naked BoHc/A or control PBS. **d**, Strong BoNT/A-specific serum IgG antibody responses were induced by intranasal immunization with cCHP-BoHc/A. **e**,**f**, Mice intranasally vaccinated with cCHP-BoHc/A were completely protected from both intraperitoneal challenge with BoNT/A and intranasal exposure to the progenitor toxin.

imaging study using small-animal positron emission tomography (PET) and X-ray computed tomography showed clearly that intranasally administered cCHP nanogel carrying [^{18}F]-labelled BoHc/A was effectively delivered to, and continuously retained by, the nasal mucosa. In contrast, most of the [^{18}F]-labelled BoHc/A administered intranasally without cCHP nanogel disappeared from the nasal cavity within 6 h (Fig. 1b and Supplementary Fig. S5). A direct counting assay using a different radioisotope [^{111}In] with a long half-life (2.805 days) further demonstrated that BoHc/A was retained in the nasal cavity for more than two days when administered intranasally with cCHP nanogel (Fig. 1c).

To explore the efficacy of cCHP nanogel as a new adjuvant-free delivery vehicle for intranasal vaccination, we next tested whether intranasal immunization with cCHP–BoHc/A would effectively induce BoNT/A-specific mucosal IgA antibody responses. A histochemical study showed that the numbers of IgA-committed B cells markedly increased in the lamina propria and paranasal sinuses of the nasal passages on intranasal immunization with cCHP–BoHc/A, but not with naked BoHc/A or control PBS (Fig. 2a). A subsequent enzyme-linked immunosorbent spot study analysing mononuclear cells isolated from the nasal cavities of cCHP–BoHc/A-immunized mice directly confirmed induction of BoNT/A-specific IgA-producing cells (Fig. 2b). Furthermore, high titres of BoNT/A-specific IgA antibodies were detected in only those nasal washes collected from mice immunized with cCHP–BoHc/A, not with naked BoHc/A or control PBS (Fig. 2c).

As mucosal vaccination induces two-layered immunity (that is, in both the systemic and the mucosal compartments)[2,4], our next experiments were designed to determine whether BoNT/A-specific serum antibody responses were induced by intranasal immunization with cCHP–BoHc/A. Vigorous BoNT/A-specific serum IgG antibody responses were induced in cCHP–BoHc/A-vaccinated mice but not in mice immunized with naked BoHc/A or control PBS (Fig. 2d). To confirm the broad utility of this strategy with cCHP nanogel, we next evaluated the efficacy of intranasal administration of cCHP nanogel carrying a second prototype vaccine antigen, tetanus toxoid (cCHP–TT). As we expected, high titres of tetanus-toxoid-specific serum IgG as well as mucosal IgA antibodies were induced by intranasal administration of cCHP–TT (Supplementary Fig. S6). These findings indicate that the cCHP nanogel can be used universally as a new protein antigen delivery vehicle for intranasal vaccines.

We next carried out toxin-challenge experiments to confirm the ability of intranasal immunization with cCHP–BoHc/A to

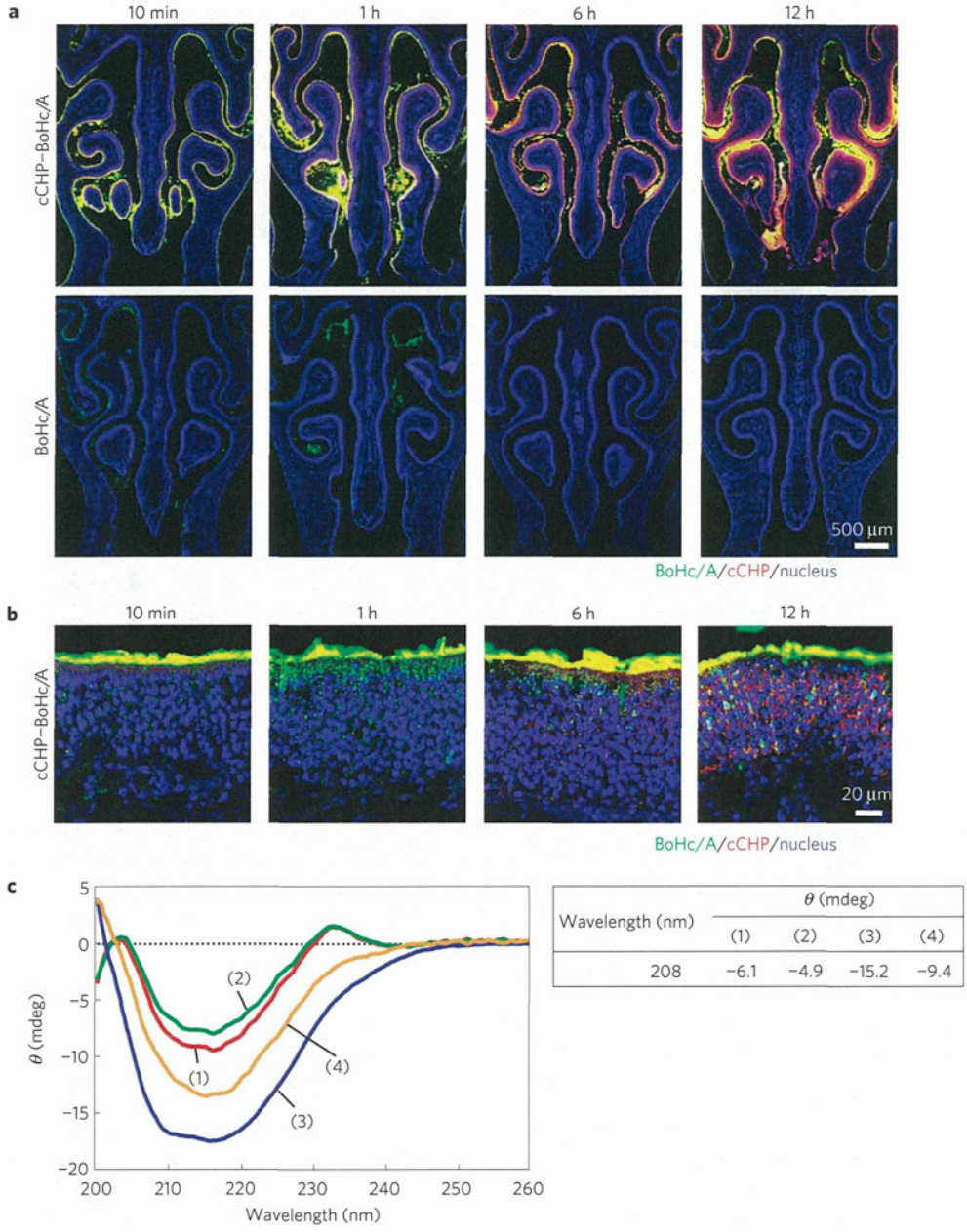

Wavelength (nm)	θ (mdeg)			
	(1)	(2)	(3)	(4)
208	−6.1	−4.9	−15.2	−9.4

Figure 3 | Chaperone-like activity of cCHP nanogel facilitates effective delivery of vaccine antigen into the nasal mucosa. a, Intranasally administered cCHP-BoHc/A but not naked BoHc/A was effectively attached to the apical membrane of nasal epithelium. **b**, BoHc/A was subsequently released from the cCHP nanogel and transported into the epithelial layer. **c**, Circular dichroism analysis showed that the ellipticity (θ) value of BoHc/A, which was decreased to −15.2 mdeg after the BoHc/A was incorporated into cCHP nanogel, recovered to −9.4 mdeg after the release of BoHc/A from the cCHP nanogel by treatment with methyl-β-cyclodextrin. (1) Native BoHc/A, (2) BoHc/A heated for 5 h at 45 °C, (3) BoHc/A incubated with cCHP nanogel for 5 h at 45 °C, (4) cCHP-BoHc/A treated with methyl-β-cyclodextrin for 1 h at 25 °C.

neutralize BoNT/A and its progenitor *in vivo*. BoNT produced by *C. botulinum* usually forms a large complex called progenitor toxin with non-toxic accessory components, such as haemagglutinin, which are involved in binding to the mucosal epithelium[32]. It has been suggested that, on infection, the progenitor toxin binds to the mucosal epithelium; BoNT/A is then released into the blood circulation after detaching from these accessory components and finally interacts with nerve cells, causing botulism[33]. After intraperitoneal (i.p.) challenge with BoNT/A (500 ng, 5.5×10^4 i.p. LD_{50}, where LD_{50} represents the dose lethal to 50% of animals tested), mice intranasally immunized with cCHP–BoHc/A survived without any clinical signs, whereas those that had received naked BoHc/A or control PBS almost immediately developed neurological signs and died within half a day (Fig. 2e). Furthermore, mice intranasally immunized with cCHP–BoHc/A were completely protected from the effects of intranasal exposure to the progenitor toxin (10 μg, 2×10^5 i.p. LD_{50}) (Fig. 2f). Thus, the intranasal vaccine formulation of cCHP–BoHc/A effectively induces both systemic and mucosal protective immunity against lethal exposure to both BoNT/A and its progenitor without the co-administration of mucosal adjuvant.

To directly address how cCHP nanogel initiates and accelerates the immune responses against incorporated vaccine antigen without the use of a mucosal adjuvant, we next carried out a series of histochemical studies with tetramethylrhodamine isothiocyanate (TRITC)-conjugated cCHP nanogel carrying Alexa-Fluor-647-conjugated BoHc/A. As we expected, within 1 h of intranasal

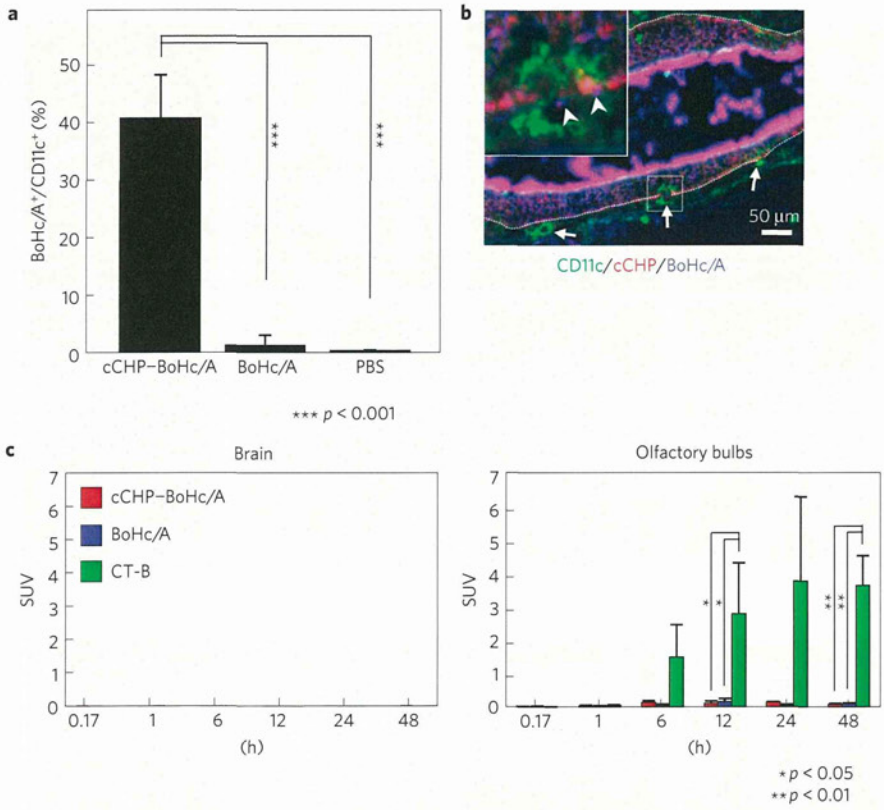

Figure 4 | Antigen delivered to dendritic cells by cCHP nanogel stimulates the nasal immune system but does not accumulate in the CNS. a,b, Flow cytometric (**a**) and immunohistochemical analyses (**b**) showed that BoHc/A released from cCHP nanogel was effectively taken up by CD11c$^+$ dendritic cells located in the epithelial layer and lamina propria of the nasal cavity, as shown by arrowheads. CD11c$^+$ dendritic cells and the basal layer of nasal epithelium in **b** are shown by arrows and dotted lines, respectively. **c**, The radioisotope counting assay showed that intranasally administered cCHP nanogel carrying [^{111}In]-labelled BoHc/A did not accumulate in the olfactory bulbs or brain. In contrast, [^{111}In]-labelled cholera toxin B subunit (CT-B), used as a positive control, accumulated in the olfactory bulbs from 6 h after administration.

administration, antigen-coupled fluorescence signals were observed in antigen-sampling M cells recognized by our previously established monoclonal antibody NKM 16-2-4 (ref. 34), in the nasopharynx-associated lymphoid tissues, which are inductive tissues for the airway mucosal immune system[4] (Supplementary Fig. S7a). However, because the nasal epithelium is anatomically widespread, cCHP–BoHc/A was universally distributed in the apical membrane of the nasal epithelium, and its density was much greater than that detected in the follicle-associated epithelium of nasopharynx-associated lymphoid tissues (Fig. 3a and Supplementary Fig. S7b). Examination of high-magnification images revealed that the cCHP–BoHc/A was internalized into the nasal epithelium immediately after the intranasal administration; BoHc/A was then detached gradually from the cCHP nanogel in a controlled manner in the nasal epithelial cells (Fig. 3b). In this regard, we previously showed that the proteins encapsulated by nanogels were released by protein exchange in the presence of excess amounts of other proteins, such as cellular components or enzymes[31]. In fact, the *in vitro* circular dichroism analysis showed that the secondary structure of BoHc/A was changed after the molecule was incorporated into the CHP nanogel but recovered after it was released (Fig. 3c). These results suggest that the cCHP nanogel acts as an artificial chaperone for intranasal vaccine antigen, leading to the induction of antigen-specific respiratory immune responses. In support of our hypothesis, the flow cytometric and immunohistochemical analyses showed that, within 6 h after administration of the BoHc/A with cCHP nanogel, the BoHc/A released from the nasal epithelium by exocytosis was effectively taken up by CD11c$^+$ dendritic cells located in both the epithelial layer and the lamina propria of the nasal cavity (Fig. 4a,b). It should be emphasized that the immunological role of cCHP nanogel is just to convey the vaccine antigen into the respiratory immune system effectively; it does not provide adjuvant-like activity to dendritic cells, because the bone-marrow-derived naive dendritic cells cultivated with cCHP nanogel did not enhance the expression of the co-stimulatory and antigen-presentation molecules (Supplementary Fig. S8). Moreover, nasal dendritic cells spontaneously expressed these molecules, probably because of chronic stimulation by inhaled environmental antigens, and their expression levels were not changed by intranasal administration with cCHP–BoHc/A (Supplementary Fig. S9). Therefore, the optimum antigen delivery offered by cCHP nanogel to activated nasal dendritic cells over a wide area of the nasal mucosa would be an effective strategy for inducing antigen-specific protective immune responses.

As the most important issue in intranasal vaccine development is to overcome safety concerns about the potential dissemination of intranasal vaccine antigens to the central nervous system (CNS), we carried out an *in vivo* tracer study with [^{111}In]-labelled BoHc/A. When cCHP nanogel carrying [^{111}In]-labelled BoHc/A was administered intranasally, no transition into the olfactory bulbs or brain was observed over a two-day period after administration (Fig. 4c). In contrast, when [^{111}In]-labelled cholera toxin B subunit, which can reach and accumulate in olfactory tissues[11], was administered intranasally with the same dose of radioisotope as used with the cCHP–BoHc/A, the radioisotope count in the olfactory bulbs was significantly higher than with cCHP nanogel holding [^{111}In]-labelled BoHc/A (Fig. 4c). These results support the hypothesis that cCHP nanogel administered intranasally possesses

no risk of redirecting the vaccine antigen into the CNS when administered intranasally and, therefore, can be used as a safe delivery vehicle for intranasal vaccines.

In essence, the nanogel antigen delivery system now opens up a new avenue for the creation of adjuvant-free intranasal vaccines. Taken in terms of its validity in leading to the induction of effective immune responses at both systemic and mucosal compartments without a concern for the deposition of vaccine antigen into the CNS, it would provide a unique and attractive vaccine strategy for the control of respiratory infectious diseases (for example, influenza).

Methods

Animals. Female BALB/c mice between 6 and 8 weeks old were maintained in the experimental animal facilities at the Institute of Medical Science of The University of Tokyo and at Hamamatsu Photonics K.K. All experiments were carried out according to the guidelines provided by the Animal Care and Use Committees of the University of Tokyo and Hamamatsu Photonics K.K.

Preparation of nanogel vaccine. CHP or cCHP nanogel synthesized as described previously[31,35] was mixed for 5 h at 45 °C at a 1:1 molecular ratio with vaccine antigen (BoHc/A expressed by *E. coli* or tetanus toxoid; kindly provided by the Research Foundation for Microbial Diseases of Osaka University). The FRET was determined by an FP-6500 fluorescence spectrometer (Jasco) with fluorescein isothiocyanate (FITC)-conjugated BoHc/A and TRITC-conjugated CHP or cCHP nanogel. The DLS of CHP or cCHP carrying, or not carrying BoHc/A, and the zeta-potential of BoHc/A with or without cCHP nanogel were determined with a Zetasizer Nano ZS instrument (Malvern Instruments). The circular dichroism spectra of BoHc/A before and after being incorporated into the cCHP nanogel, and after release from the cCHP nanogel by treatment with 15 mM of methyl-β-cyclodextrin, were obtained by using a J-720 spectropolarimeter (Jasco). To determine the cellular uptake *in vitro*, HeLa cells were treated with 10 nM of CHP or cCHP nanogel carrying FITC-conjugated BoHc/A, or of FITC-conjugated naked BoHc/A, for 4 h and analysed by flow cytometry with FACSCalibur (Becton Dickinson).

***In vivo* imaging study and radioisotope counting assay.** cCHP nanogel incorporating [^{18}F]-labelled BoHc/A was administered intranasally to mice and the distribution of radioisotope in the nasal cavity was determined by using a small-animal PET system (Clairvivo PET, Shimadzu Corporation)[36]. The radioisotope signals were measured for 10 h after administration and were superimposed on the image obtained by a small-animal X-ray computed tomography scanner (Clairvivo CT, Shimadzu Corporation). The images were analysed by using a PMOD software package (PMOD Technologies) and expressed as standardized uptake values (SUV) calculated from radioactivity in the volumes of interest. To trace the antigen for longer, [^{111}In]-labelled naked BoHc/A was administered intranasally with or without cCHP nanogel and the radioisotope counts in the nasal mucosa, olfactory bulbs and brain were directly measured by a γ-counter (1480 WIZARD, PerkinElmer) 10 min, 1, 6, 12, 24 and 48 h after administration. As a control, [^{111}In]-labelled cholera toxin B subunit[37] was administered intranasally. SUV was calculated as radioactivity (c.p.m.) per gram of tissue divided by the ratio of injection dose (1×10^6 c.p.m.) to body weight.

Immunization study. CHP or cCHP nanogel (each 88.9 μg for BoHc/A or 78.5 μg for tetanus toxoid) carrying BoHc/A (10 μg) or tetanus toxoid (30 μg), or the same amount of naked BoHc/A or tetanus toxoid dissolved in 15 μl of PBS, was administered intranasally to mice on three occasions at 1-week intervals. Sera were collected before, and 1 week after, each immunization, and nasal wash samples were taken 1 week after final immunization for antigen-specific enzyme-linked immunosorbent assay as described previously[34,38]. Mononuclear cells were isolated from the nasal passages 1 week after the final immunization and subjected to antigen-specific enzyme-linked immunosorbent spot analysis as shown in a previous study[38].

Neutralizing assay. To analyse the toxin-neutralizing activity of cCHP–BoHc/A-induced serum IgG and nasal IgA antibodies, the immunized mice were intraperitoneally challenged with 500 ng of BoNT/A (5.5×10^4 i.p. LD_{50}) diluted in 100 μl of 0.2% gelatin/PBS or intranasally exposed to 10 μg (in 10 μl PBS, 5 μl per nostril) of *C. botulinum*type-A progenitor toxin (2×10^5 i.p. LD_{50}, Wako). Clinical signs and survival rates were observed for 7 days, as described previously[34,38].

Histochemistry and flow cytometric analyses. Frozen sections of nasal tissues prepared from immunized mice were stained with FITC-conjugated anti-mouse IgA (BD Biosciences). To determine the distribution of cCHP–BoHc/A after intranasal administration, either TRITC-conjugated cCHP nanogel carrying Alexa-Fluor-647-conjugated BoHc/A, or Alexa-Fluor-647-conjugated naked BoHc/A, was administered intranasally and the sections of nasal tissues were stained with FITC-conjugated NKM 16-2-4 (ref. 34) or biotinylated anti-CD11c (BD Biosciences). For CD11c staining, the sections were then treated with streptavidin/horseradish peroxidase diluted 1:1000 (Pierce) followed by tyramide–FITC (PerkinElmer Life and Analytical Sciences). All sections were finally counterstained with 4,6-diamidino-2-phenylindole (Sigma) and analysed under a confocal laser-scanning microscope (TCS SP2, Leica) or a fluorescence microscope (BZ-9000, Keyence). To determine the antigen uptake by dendritic cells, cCHP nanogel carrying Alexa-Fluor-647-conjugated BoHc/A, Alexa-Fluor-647-conjugated naked BoHc/A or control PBS was administered intranasally. After 6 h, mononuclear cells were isolated from the nasal passages and stained with FITC-conjugated CD11c (BD Biosciences). The frequency of BoHc/A$^+$ CD11c$^+$ cells was analysed by flow cytometry.

Data analysis. Data are expressed as means ± standard deviation. All analyses for statistically significant differences were carried out by Tukey's t-test, with significance indicated by p values of <0.001 (***), <0.01 (**) and <0.05 (*).

Received 9 December 2009; accepted 10 May 2010; published online 20 June 2010; corrected online 2 July 2010

References

1. Wagner, V., Dullaart, A., Bock, A. K. & Zweck, A. The emerging nanomedicine landscape. *Nature Biotechnol.* **24,** 1211–1217 (2006).
2. Holmgren, J. & Czerkinsky, C. Mucosal immunity and vaccines. *Nature Med.* **11,** S45–S53 (2005).
3. Varmus, H. *et al.* Public health. Grand challenges in global health. *Science* **302,** 398–399 (2003).
4. Kiyono, H. & Fukuyama, S. NALT- versus Peyer's-patch-mediated mucosal immunity. *Nature Rev. Immunol.* **4,** 699–710 (2004).
5. Belshe, R., Lee, M. S., Walker, R. E., Stoddard, J. & Mendelman, P. M. Safety, immunogenicity and efficacy of intranasal, live attenuated influenza vaccine. *Exp. Rev. Vaccines* **3,** 643–654 (2004).
6. Lavelle, E. C. Generation of improved mucosal vaccines by induction of innate immunity. *Cell. Mol. Life Sci.* **62,** 2750–2770 (2005).
7. Yuki, Y. & Kiyono, H. New generation of mucosal adjuvants for the induction of protective immunity. *Rev. Med. Virol.* **13,** 293–310 (2003).
8. Xu-Amano, J. *et al.* Helper *T* cell subsets for immunoglobulin A responses: Oral immunization with tetanus toxoid and cholera toxin as adjuvant selectively induces Th_2 cells in mucosa associated tissues. *J. Exp. Med.* **178,** 1309–1320 (1993).
9. Takahashi, I. *et al.* Mechanisms for mucosal immunogenicity and adjuvancy of *Escherichia coli* labile enterotoxin. *J. Infect. Dis.* **173,** 627–635 (1996).
10. Mutsch, M. *et al.* Use of the inactivated intranasal influenza vaccine and the risk of Bell's palsy in Switzerland. *New Engl. J. Med.* **350,** 896–903 (2004).
11. van Ginkel, F. W., Jackson, R. J., Yuki, Y. & McGhee, J. R. Cutting edge: The mucosal adjuvant cholera toxin redirects vaccine proteins into olfactory tissues. *J. Immunol.* **165,** 4778–4782 (2000).
12. Reddy, S. T., Swartz, M. A. & Hubbell, J. A. Targeting dendritic cells with biomaterials: Developing the next generation of vaccines. *Trends Immunol.* **27,** 573–579 (2006).
13. Peek, L. J., Middaugh, C. R. & Berkland, C. Nanotechnology in vaccine delivery. *Adv. Drug Deliv. Rev.* **60,** 915–928 (2008).
14. Sharma, S., Mukkur, T. K., Benson, H. A. & Chen, Y. Pharmaceutical aspects of intranasal delivery of vaccines using particulate systems. *J. Pharm. Sci.* **98,** 812–843 (2009).
15. Oh, J. K., Drumright, R., Siegwart, D. J. & Matyjaszewski, K. The development of microgels/nanogels for drug delivery applications. *Prog. Polym. Sci.* **33,** 448–477 (2008).
16. Reamdonck, K., Demeester, J. & Smedt, S. D. Advanced nanogel engineering for drug delivery. *Soft Matter* **5,** 707–715 (2009).
17. Morimoto, N., Nomura, S., Miyazawa, N. & Akiyoshi, K. Nanogel engineered design for polymeric drug delivery. *Polym. Drug Deliv.* **II,** 88–101 (2006).
18. Akiyoshi, K., Deguchi, S., Moriguchi, N., Yamaguchi, S. & Sunamoto, J. Self-aggregates of hydrophobized polysaccharides in water. *Macromolecules* **26,** 3062–3068 (1993).
19. Akiyoshi, K., Deguchi, S., Tajima, T., Nishikawa, T. & Sunamoto, J. Microscopic structure and thermoresponsiveness of a hydrogel nanoparticle by self-assembly of a hydrophobized polysaccharide. *Macromolecules* **30,** 857–861 (1997).
20. Nomura, Y., Ikeda, M., Yamaguchi, N., Aoyama, Y. & Akiyoshi, K. Protein refolding assisted by self-assembled nanogels as novel artificial molecular chaperone. *FEBS Lett.* **553,** 271–276 (2003).
21. Uenaka, A. *et al. T* cell immunomonitoring and tumor responses in patients immunized with a complex of cholesterol-bearing hydrophobized pullulan (CHP) and NY-ESO-1 protein. *Cancer Immun.* **7,** 9 (2007).
22. Kageyama, S. *et al.* Humoral immune responses in patients vaccinated with 1-146 HER2 protein complexed with cholesteryl pullulan nanogel. *Cancer Sci.* **99,** 601–607 (2008).
23. Nishikawa, T., Akiyoshi, K. & Sunamoto, J. Macromolecular complexation between bovine serum albumin and the self-assembled hydrogel nanoparticle of hydrophobized polysaccharides. *J. Am. Chem. Soc.* **118,** 6110–6115 (1996).